

Experimentally, analytically, and numerically investigation of punching shear behaviour of edge-flat slab column connections with different opening numbers

Hanaa gamal Mohammed

Civil engineering, Elnahda university, Beni Suef

Naglaa Jalal Al-Din ,fahmy

civil engineering, Higher Institute of Engineering and Technology New Minia,
Egypt

Lailah mahmoued, soliman

Faculty of Engineering, El-Minia University, Egypt

Alaa Youssef, Abouelezz,

Faculty of Engineering, El-Minia University, Egypt

Abstract:

The versatility of a flat slab system's design makes it popular. Openings might really be necessary to connect to public services like gas lines or deflation. In most cases, the designer has no control over where these openings must be placed in relation to or even directly next to the supporting column. In this case, the discontinuity between the concrete and reinforcing steel created by openings and flat slabs, particularly those with edge columns, is more susceptible to punching problems. The ability of a concrete slab's cross-section to withstand punching shear has an impact on that capacity. Openings that negatively affect flat slab punching shear behaviour are experimentally investigated on two specimens with different opening numbers in this research. Experimental results were used to determine the maximum load, deflection, energy absorption, and stiffness. The experimental results were compared with both the theoretical results using ANSYS V.21 software and the analytical results using Egyptian and American codes.

The experimental results showed that holes in the critical perimeter surrounding columns reduce flat slabs' punching shear resistance. The decrease is inversely related to column face opening number and location. Punching capability diminishes with more openings, especially from one to two.

In the slab with two openings, the ACI 318-19 code had higher maximum load values than the experimental values, but in the other cases, the maximum load values were lower. ANSYS V.21 numerical results match experimental results. The experimental results and the numerical findings produced using ANSYS V.21 agree rather well.

Keywords: Flat-slab, Edge-column, Punching, Openings; Ansysv.21, ECP 203-2020, ACI 318-19,

1. Introduction

Flat slabs are frequently used in construction because of their quick installation, versatility in design, and cost benefits [1–2]. As they are supported by columns without drop panels, it is possible to reduce the height of the building and easily change interior layouts. Globally, effective design methods and tools for flat slab building have been developed because of thorough research. This structural system's main flaw is that it is susceptible to punching shear failure, a brittle mode that frequently happens without any warning because of small deflections and hidden cracks. A local punching shear failure at column may spread to surrounding columns, eventually causing the whole structure to progressively collapse [3–4]. During the design phase, punching shears must be thoroughly studied and any design must be on the safe side. However, due to a lack of experimental data, the effects of slab openings on punching shear behaviour are often neglected or approximate solutions are used. There is a need for more research into the punching shear behaviour of slabs because of how a slab's opening is sized and positioned relative to the supporting column. For architectural reasons, such as the installation of stairways or lifts or to provide gas, electricity, water and air conditioning systems, slabs can include openings of different sizes. Additionally, slab openings may be placed close to or faraway from vertical load-resisting columns. It is essential to do a detailed analysis of how these slab openings may affect punching shear behaviour.

Several design considerations can be considered to prevent brittle punching shear failure, including reducing loads, reducing slab dimensions, increasing slab thickness, reinforcing the intersection of columns and slabs, and increasing column diameters. However, due to architectural limitations, these steps might not always be feasible. In these situations, shear reinforcement at the intersection of the column and slab may improve ductility and strength while reducing the possibility of brittle failure.

Numerous experiments have been done to determine how the opening size and position affect the behaviour of punching shear in reinforced concrete (RC) flat slabs. El-Shafiey et al. studied the effect of openings and found that specimens with openings had a much lower punching shear capacity than control slabs, with reductions ranging from 20.61 to 50.82 %. Anil et al. tested two-way RC flat slabs with different sizes and positions of openings. They discovered that increasing the opening led to a decrease in punching shear capacity, especially for openings close to columns where the reduction was more pronounced. For slabs with 500x500 mm openings, the ultimate capacity fell to around 40%. Elsayed et al. [7] investigated the effect of crumb rubber in slabs with openings and showed that openings close to column sides reduced punching shear capacity by approximately 24% for 100x100 mm holes and 35% for 150x150 mm openings. With regard to solid slabs, Liberati et al. [8] investigation on shear failure on flat slabs near columns showed significant losses in ultimate capacity, stiffness, and energy dissipation. In order to determine the effect of openings in RC slabs without shear reinforcement, Genikomsou and Polak [9] created a finite element model, which they used to confirm that punched shear resistance decreased as opening size grew. By using a finite element model to analyze the effects of openings in various locations and sizes, Mostofinejad et al. [10] discovered that openings close to columns greatly enhanced the shear stress around the slab-column connections. Teng et al. [11] investigated the

punching shear behaviour of two-way RC slabs with openings supported on rectangular columns, concluding that openings decreased punching strength significantly, with the ideal location for openings being along the column's longer side. International building codes, such as ECP 203-2020 [12] and ACI 318-19 [13], differ nearly significantly in their approaches, particularly in determining the critical punching perimeter, which varies from $0.50d$, where 'd' represents the effective depth of the slab. This difference has a significant effect on the slab's capacity, especially in the presence of openings. These codes also varied in how they determined the critical punching perimeter reduction owing to openings, with some utilizing tangent lines drawn from the loaded area's center to the opening corners. The distance between an opening and the face of the column is limited by ACI 318-19 [13]. According to ACI 318-19 [13], the minimum distances from the column face are $4d$ (where "d" and "H" measure the effective slab depth and slab thickness, respectively). The ECP203-2020 [12] prefers not to create an opening adjacent to a column face. It established constraints and criteria for constructing apertures in a flat slab. The maximum size of an aperture at the intersection of two middle strips is equal to 0.4 of the spans. Openings are constructed at the intersection of a column strip, and a middle strip can have a maximum dimension of 1/4 of the span. Finally, the opening is located where two column strips meet and has a maximum dimension equal to 0.1 of the spans.

This paper studied the punching shear behavior of flat slabs with an edge column connection and opening dimensions that are larger than what international codes recommend. The parameters included different opening numbers and locations. The main parameter is the negative effect of openings (one or two openings). Comparisons between experimental results, numerical ANSYSV.21, and analytical results from two different codes are presented in this research.

2. Experimental program

Two edge-column flat-slab connections were prepared with dimensions of 1500 x 1000 x 120 mm and tested under vertical load. The square edge column dimensions are 200x200mm, with 400 mm total height. Figs. 1–2 describe the layout of the slabs with one and two openings. Slabs were reinforced with 6 \varnothing 12/m at the bottom and 6 \varnothing 10/m at the top to prevent flexural failure, which was designed according to ECP 203-2020 [12]. The column is reinforced with 4 \varnothing 12 longitudinal steel and 6 \varnothing 8/m stirrups. The reinforcement details of the two slabs are shown in Figs. 3–4.

The experimental program was divided into two slabs to study the negative effect of openings in flat slabs on the ultimate slab punching shear capacity. Two slabs were used, one with one opening and the other with two openings. Opening dimensions of 200 mm x 200 mm in two flat slabs are more than the maximum dimension recommended by ECP 203-2020 [12] ($\text{span}/10$). Table 1 depicts the details of the testing slabs.

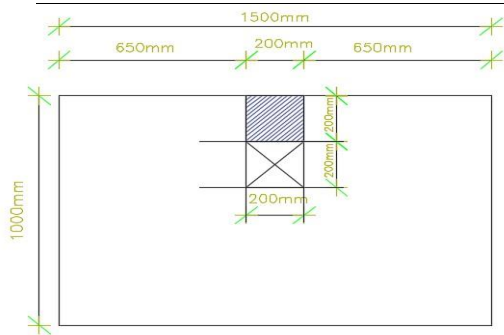


Fig. 1: Layout of slab with one opening

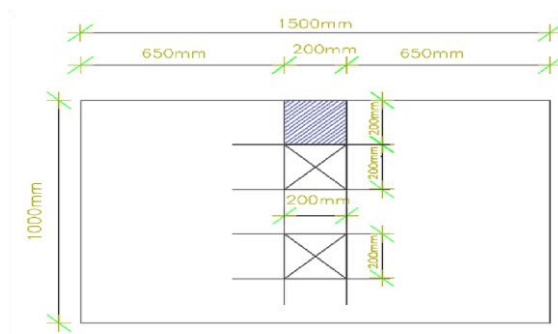


Fig. 2: Layout of slab with two openings

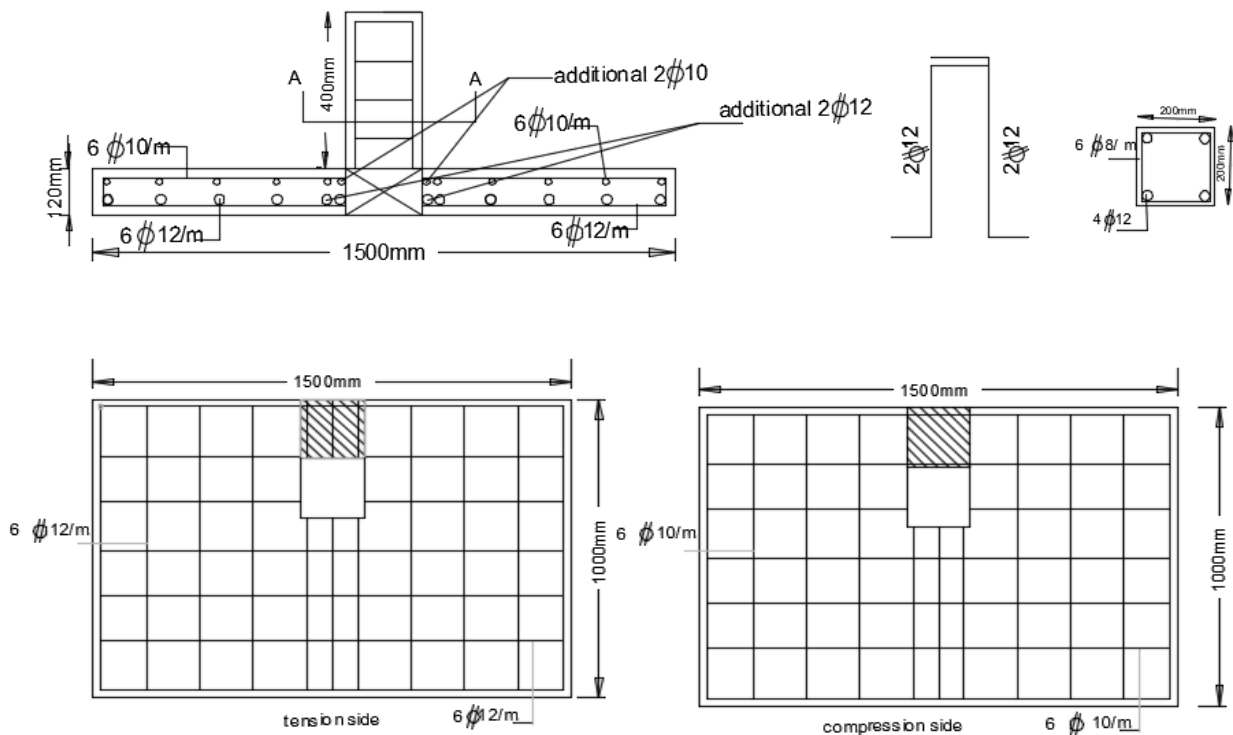


Fig.3. Reinforcement details of specimen with one opening

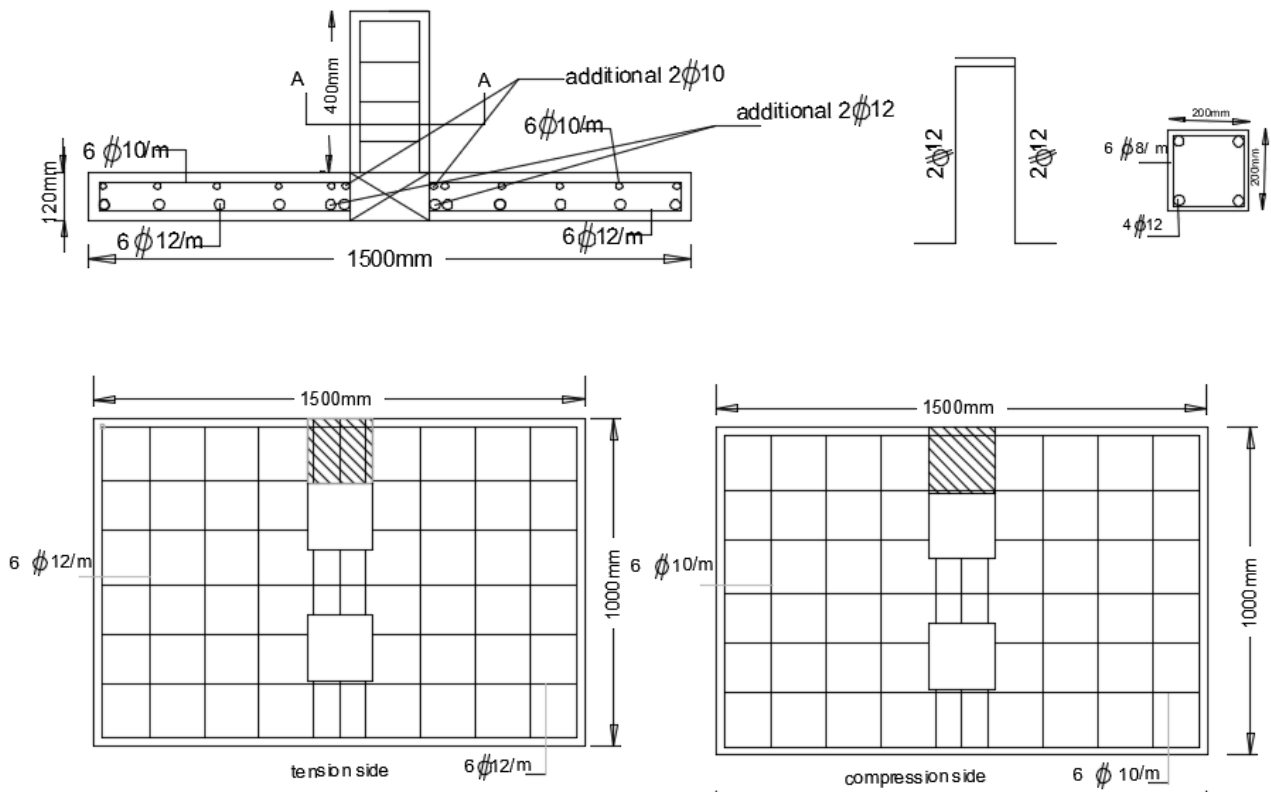


Fig.4. Reinforcement details of specimen with two openings

Table 1: Details of experimental specimens

Specimen symbol	Specimen name	Slab dimension	Slab reinforcement of top and bottom	Opening Number	Opening Dimensions	Column dimensions /reinforcement
S-A-O	slab with one opening.	1500*1000*120mm	Top 6 Ø 10/m Bottom 6 Ø 12/m	1	200*200mm	200*200mm 4 Ø 12 longitudinal steel, 6 Ø 8/m stirrups.
S-A-2O	slab with two openings.			2		

3. Material Properties and Mixture Proportion

3.1 Material Properties

The concrete mix components included Sinai Cement Company's Ordinary Portland Cement (grade 52.5 MPa), which complied with ES 4756/1-2020 [14] and had a specific gravity of 3.15. The crushed dolomite from the Ataq mountain quarry used to make the coarse aggregate had a maximum size of particles of 20 mm and a specific gravity of 2.7. As the final component, clean, silt- and clay-free natural sand with a specific gravity of 2.63 was employed. Following ES 262/2015 [15], high-grid steel (360/520 yield stress/ultimate stress) of 10 and 12mm diameters, together with mild steel grade 280/450 for stirrups, were used. Table 2 provides a summary of the mechanical qualities.

Table 2. Properties of reinforcement used in the experimental work.

Properties	Φ 8	Φ 10	Φ 12
Yield stress (MPa)	280	488.7	524.7
Ultimate Stress (MPa)	388	660	697.4
Actual Area (mm^2)	50 .27	78.54	113.1

3.2 Mix design

To achieve an average cube-crushing strength of 28 MPa after 28 days, a concrete mixture has been created (f_{cu})(cubic compressive strength). Six concrete cubes were used to test the concrete's strength after 28 days. Information on the mixed proportions by weight of the ingredients is illustrated in Table 3.

Table 3. Mix Design Proportion (Average Strength=28MPa)

Material	Basalt	Sand	Cement	Water
Mix Proportion Kg/m ³	1160	580	400	180

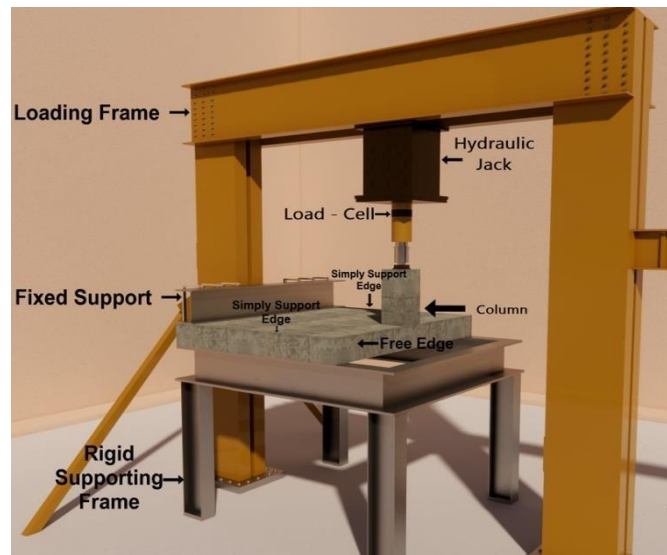
:

4. Test setup and instrumentation

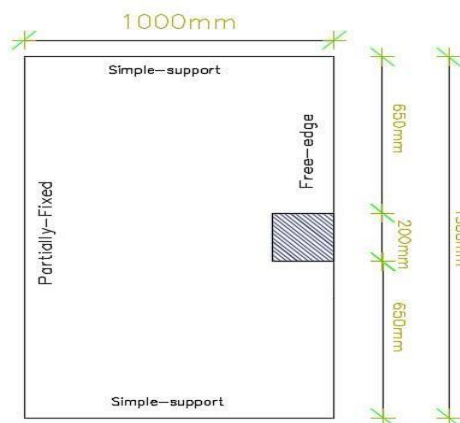
The slabs were tested in the reinforced concrete laboratory of Al-Azhar University's College of Engineering in Egypt, using a load mechanism with a capacity of 250 KN. Fig. 5 depicts the test setup. The side of the column was left free, and the two sides perpendicular to the column were simple to maintain while the side parallel to the column was fixed. On the bottom side, a linear variable differential transformer (LVDT) was put in the middle of the slab. The LVDT in the test has a 0.1 sensitivity range of +/- 100 mm, as illustrated in Fig. 6.

Strain gauges: the strain gauges' position, which was $d/4$ from the column face (the top surface of the slab), and measured strains in the concrete to be 60 mm long.

A hydraulic jack: A load cell mounted on the column stub was used to measure the load applied by a hydraulic jack as it was applied downwardly in increments of 20 to 30 kN until failure. The strain gauge, electrical screen, and load cells' readings were all monitored.



a) Isometric-View



b) Plan View

Fig. 5: Test setup (Isometric-View, dimensions in mm)

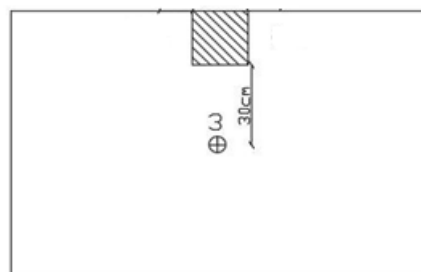


Fig. 6: LVDT location

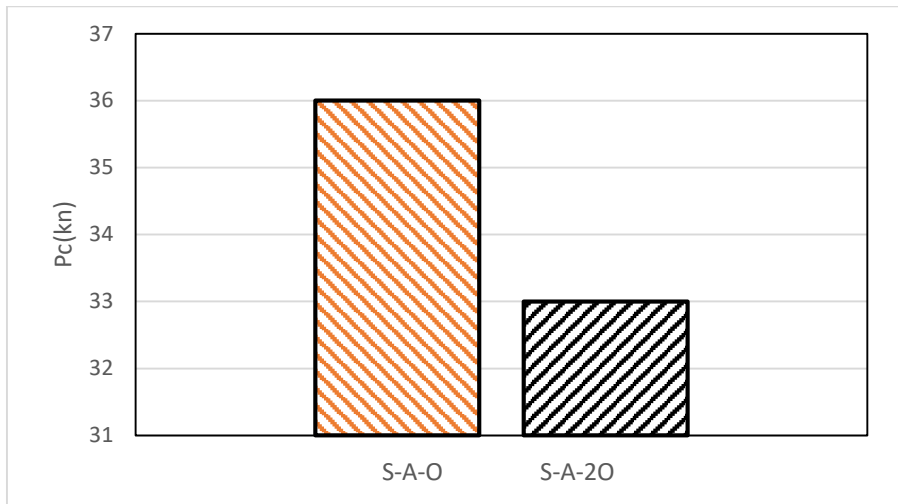


Fig. 9: Cracking load of the tested slabs

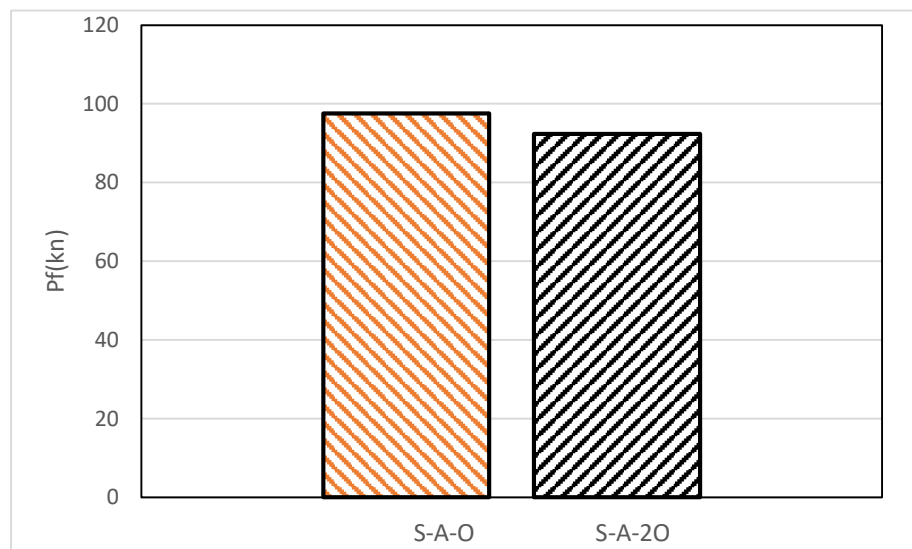


Fig. 10: Failure load of tested Slabs

5.2 Load deflection

Fig. 11 shows an increase in slab with two opening deflections compared with slab with one opening deflection at all loading stages. The increase in deflection becomes larger at the last stage of loading. This is due to the big loss of inertia owing to openings, which is a function of the slab stiffness. The increase in deflection depends on the number of openings, as the number increases, the deflection increases.

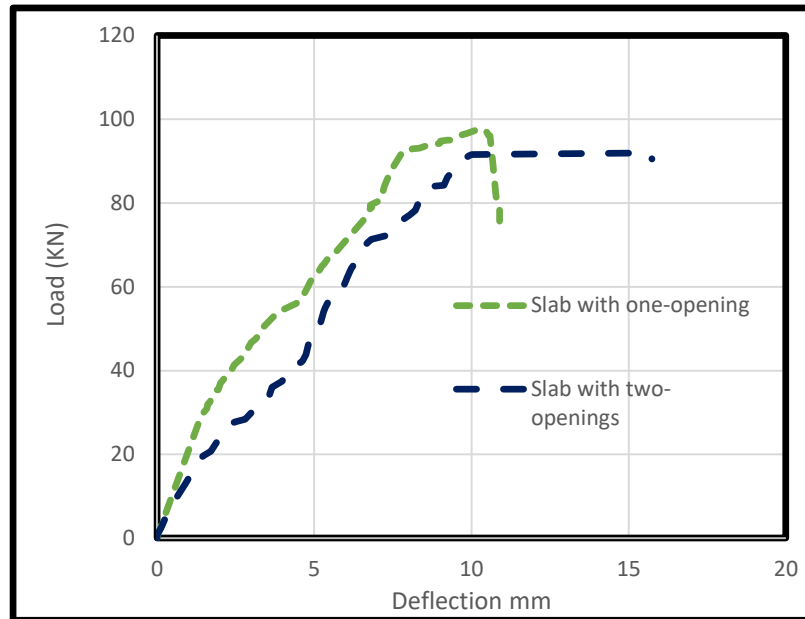


Fig. 11. Load, and deflection for two Slabs, which One, and Two-Openings

Table 4. Experimental results of the tested slabs

Specimens	Cracking stage (mm)		Ultimate stage		Stiffness	The maximum compressive concrete strain	Energy absorption (kN.mm)
	Δ_{cr} (mm)	P_{cr} (KN)	Δ_f (mm)	P_{ult} (KN)	K_i (KN/mm)	ϵ_{cu}	
S-A-O	1.94	36	10.18	97.57	12.84	0.00142	735
S-A-2O	3.42	33	15.64	92.32	9.999	0.00137	690

Δ_{cr} (mm): deflection (at the first crack).

P_{cr} (KN): cracking load (at the first crack).

k_i (KN/mm): initial stiffness

Δ_f : deflection at the ultimate load)

P_u (KN): ultimate load (at the ultimate crack).

5.3 Concrete Compressive Strain

At a distance of $d/4$ from the column face (the top surface of the slab), the load-concrete compression strain curves for all tested slabs are displayed in Fig. 12. There is a minor reduction in the concrete compressive strain of the slab with two openings compared with the slab with one opening at the same load level. This may be due to the position of the strain gauge near the column face, which is located on the other side of the opening. The ultimate concrete compression strain of the slab with two openings is lower than the ultimate concrete compression strain of the slab with one opening by about 3.52%.

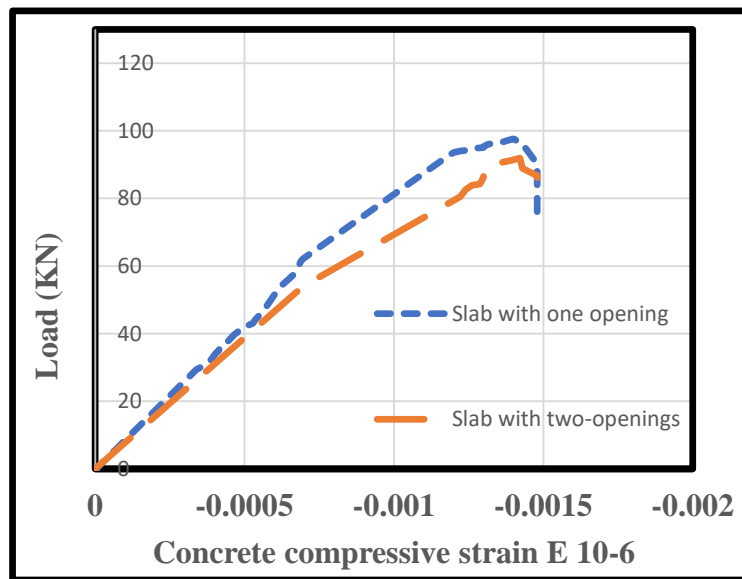


Fig. 12: Load- compressive concrete strain for the two slabs with one and two-openings

6. Analysis of results

6.1 Stiffness

The slope of the linear region of the load-deflection curve was used to determine the stiffness of the test specimens. Two slabs' initial stiffness is shown in Fig. 13. The following can be denoted about them:

There is a significant reduction in the stiffness of the slab with two openings compared with the stiffness of the slab with one opening. The reduction in stiffness was 22.4%. This confirms that the increase in openings in flat slabs increases the deflection, which is the stiffness function. As the deflection increases, the stiffness decreases.

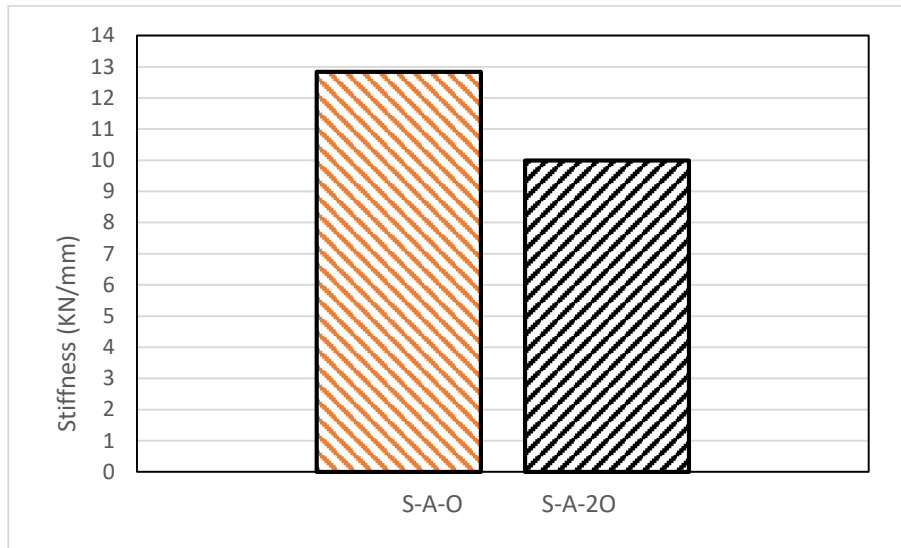


Fig. 13: Initial Stiffness Values

6.2 Energy absorption

Energy absorption was calculated using the area under the load-deflection curve, as illustrated in Fig. 14. It refers to an ability to withstand or absorb force. This calculation demonstrates how openings weaken the flat slabs. The slab with two openings has a 6.12% lower energy absorption compared to the slab with one opening.

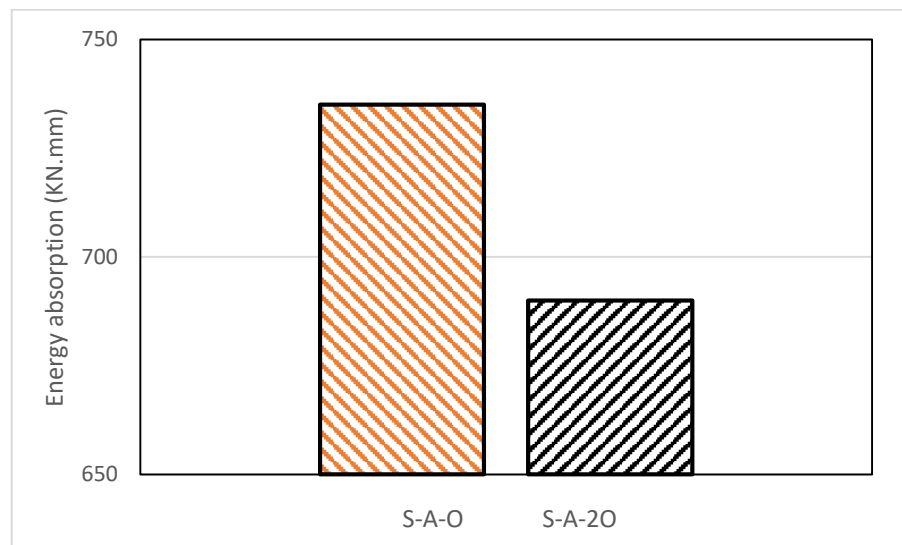


Fig. 14: Energy absorption for all specimens.

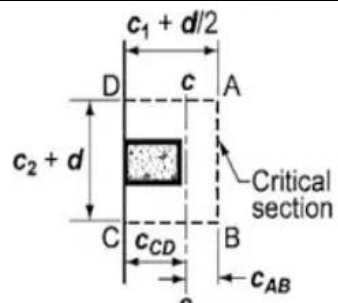
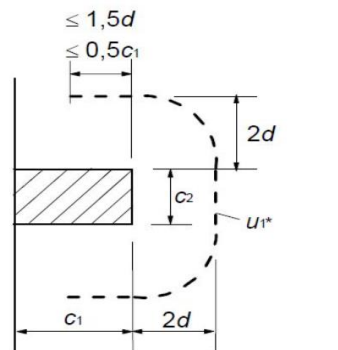
7. Comparison between Experimental results, and Analytical Predictions using ECP 203-2020[12], and ACI 318-19[13] codes

Table 5 compares the results of experimental and analytical from ECP 203-2020 and ACI 318-19 codes. Table 6 shows the equations recommended with ECP 203-2020 and ACI 318-19 codes. When comparing the experimental results to the code outcomes for the two specimens with one opening and two openings, it was discovered that the codes do not account for the presence of the second opening. This is because it is located outside the essential zone of punching around the edge column and because the two openings face the same way. Both the ECP 203-2020 and ACI 318-19 codes show lower estimated values when calculating the ultimate load, except for the ACI code when calculating the ultimate load of a slab with two openings, as shown by the comparison. The reason for this is that the second opening site is far from the area of the critical punching perimeter from the edge column which is currently embarrassing. Therefore, the resistance to sheer strength is not as drastically changed by the second vent.

Table 5: Comparison between experimental and analytical results

Specimen No	$P_{u Exp}$ (kN)	Analytical Results		$P_{u ECP} / P_{u EXP}$	$P_{u ACI} / P_{u EXP}$
		$P_{u ECP}$ (kN)	$P_{u ACI}$ (kN)		
S-A-O	97.57	81.9	93.6	0.84	0.96
SA-2O	92.32	81.9	93.6	0.89	1.01

Table 6. Summary of codes provision with proposed equation

Codes	Critical parameter	Nominal Shear Capacity	Concrete Punching shear Capacity (in concrete without shear reinforcement) (Units: N and mm)	Concrete Punching shear Capacity (in concrete with shear reinforcement) (Units: N and mm)
ECP 203-2020[36]	 <p style="text-align: center;">Critical section</p> <p style="text-align: center;">Located at 0.5d from the column's face $b_0 = 2(c_1 + d/2) + (c_2 + d)$</p>	$Q_c = \min of \begin{cases} 0.8 \left(\frac{\alpha d}{b_0} + 0.2 \right) \sqrt{f_{cu}} b_0 d \\ 0.316 \left(\frac{a}{b} + 0.5 \right) \sqrt{f_{cu}} b_0 d \\ 0.316 \sqrt{f_{cu}} b_0 d \end{cases}$	$q_{cup} = 0.316 \sqrt{\frac{f_{cu}}{\gamma_c}}$	$Q_{cups} = 0.12 \sqrt{\frac{f_{cu}}{\gamma_c}} + \phi \frac{A_{st} f_{yt}}{b_0 s}$
Eurocode [39]	 <p style="text-align: center;">Located at 2d from the column's face. $b_0 = 2(c_1 + 2d) + (c_2 + 4d)$</p>	$Q_c = \frac{0.18}{\gamma_c} \xi (100 \rho f'_c)^{\frac{1}{3}} b_0 d$ $\xi = 1 + \sqrt{\frac{200}{d}}$	$q_{cup} = C_{Rd,c} k (100 \rho f'_c)^{\frac{1}{3}} + k_1 \sigma > v_{min} + k_1 \sigma \rho$	$Q_{cups} = 0.075 q_{cup} + 1.5 \left(\frac{d}{s} \right) A_s + f_{y,eff} \left(\frac{1}{b_0 d} \right) \sin \alpha$ $f_{y,eff} = 250 + 0.25d < f_y$

8. Non-linear solution and failure criteria

Link 180 and solid elements 65 were used for the slab verification, as shown in Fig. 15. Solid 65 elements can represent tension cracking and compression crushing. The reinforcing steel was modeled using the link180 element, a two-node structural element that can replicate elements exposed to compression and tension. The slab was supported on all four sides, and the load was applied as a displacement at the column area until failure occurred. To investigate the system's behaviour, a non-linear static analysis was performed. The loads were applied progressively in 50 steps, and the entire Newton-Raphson approach was used to aid in the convergence of the analysis. The longitudinal reinforcing steel was modeled as an isotropic, elliptic-perfect plastic. The elastic modulus and Poisson's steel grade 460/660 ratio were $2e5$ MPa and 0.30, respectively. The shear transfer coefficient for a wide-open crack is 0.2. Closed cracks have a shear transfer coefficient of 0.8. Figs. 16–17 depict the numerical analysis's finite element mesh as well as the boundary of two slabs. The material properties for the concrete and reinforcing steel of the two slabs are presented in Table 7. Multiple load increments were created in this investigation from the total applied load. The convergence at the end of each load increment, within specified tolerance limits, was ensured using the Newton-Raphson equilibrium iteration method. The ANSYS V.21 program automatically determined and controlled the load step sizes while taking into account both minimum and maximum criteria. To reduce the buildup of forces throughout the iteration process, a convergence tolerance of 0.02 displacement and a maximum iteration number of 50 was set for this analysis.

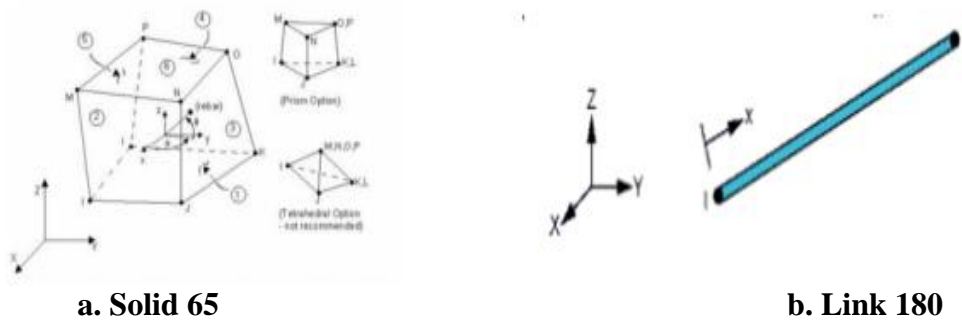


Fig. 15: Elements geometry used to model specimens

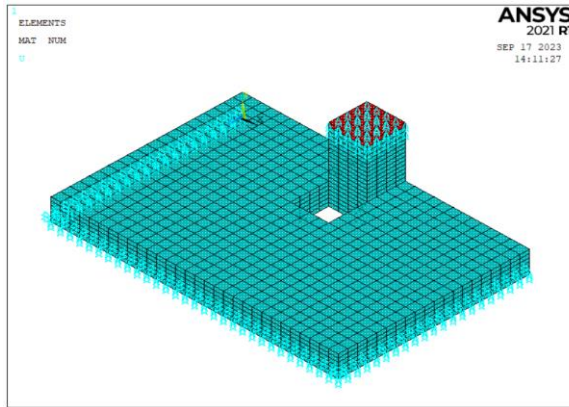


Fig. 16: A finite element mesh of specimen with one opening

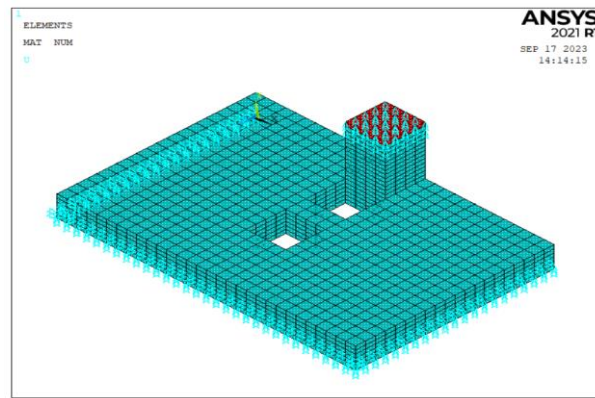


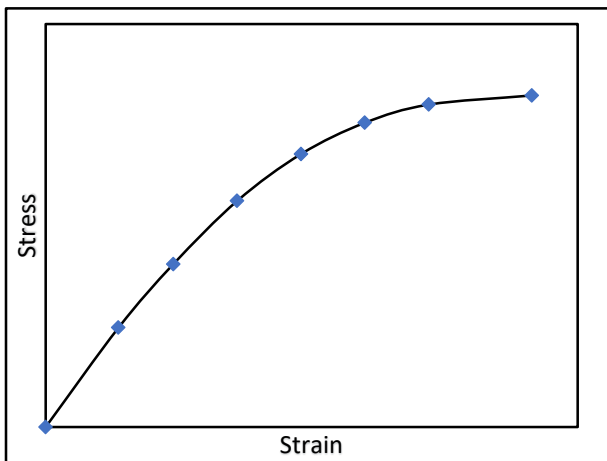
Fig. 17: A finite element mesh of specimen with two openings

Table 7: Material properties of reinforcing steel and concrete for the models

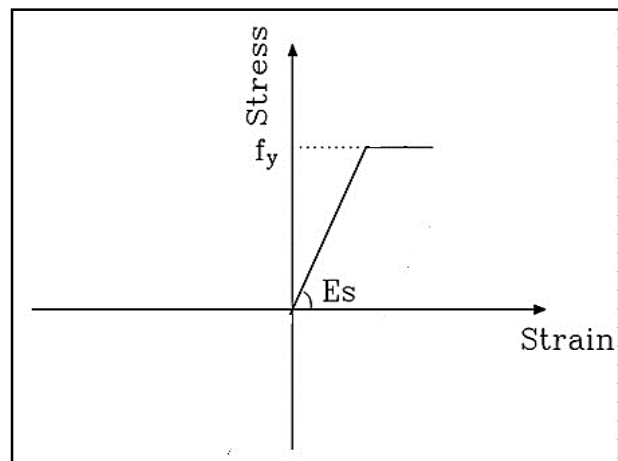
steel properties			concrete properties	
Es MPa	f_y MPa	ν	f_{Cu} MPa	ν
2e5	365	0.3	28	0.2

1. Material models

The material models employed in the experimental research of concrete and steel are depicted in a simplified form in Fig. 18. Reinforcement's stress-strain relationship is modelled by a bilinear strain-hardening yield and stress-plastic strain curve. Young's modulus of 200,000 MPa and Poisson's ratio of 0.3 characterise the elastic behaviour of the reinforcement, as was previously mentioned.



a) Material model of the concrete



b) Material model of the steel

Fig. 18: Material models for concrete, and steel reinforcement

8. Results, and discussion of the verification

The numerical results of each specimen in ANSYSV.21 were compared to the data obtained from the experimental tests. Three factors were compared between experimental work and numerical analysis: failure load, load-deflection curve, and concrete strains.

8.1 cracking load

Table 8 shows the comparison between the numerical and experimental first cracking load for the experimental slabs. The numerical first cracking load was in good agreement with those observed from test results for specimens. The first cracking load for slabs (S-A-O and S-A-2O) in the experimental test is higher than that of the numerical analysis by 10% and 4%; and the deflection increased by 7% [16].

8.2 Cracking patterns and principal strain contours

Figs. 18–19 show the cracking pattern and principal strain contours for two tested specimens close to the peak point to better identification cracks.

8.3 Ultimate load deflection Relationship

The deflection, and versus load figures showed a very close behavior. The ultimate load for slabs (S-A-O and S-A-2O) in the experimental test is higher than that of the numerical analysis by 10% and 4%; and the deflection increased by 11% and .1% respectively [16-17]., as shown in Figs. 19-20 and table 6.

Table 8: Comparison between the verification model and the experimental tested slab

Specimen	Experimental			Numerical			Num./ Exp.		
	First cracking load (kN)	Ultimate load (kN)	Defl. (mm)	First cracking load (kN)	Ultimate load (kN)	Defl. (mm)	First cracking load (kN)	Ultimate load (kN)	Defl. (mm)
S-A-O	36	97.57	10.18	38	107.37	9.2	1.06	1.10%	1.11%
S-A-2O	33	92.32	8.11	35	95.57	8.12	1.06	1.04%	.01%

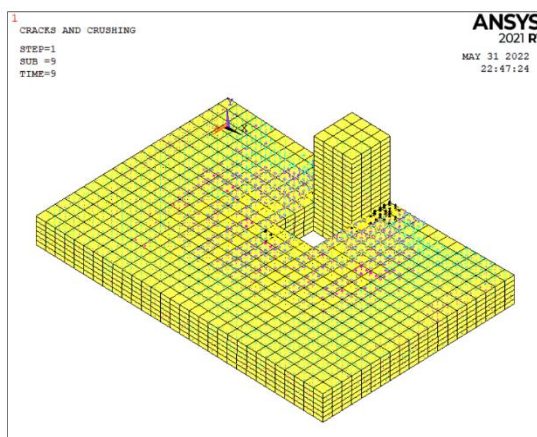


Fig. 19: Cracking pattern for specimen with one opening

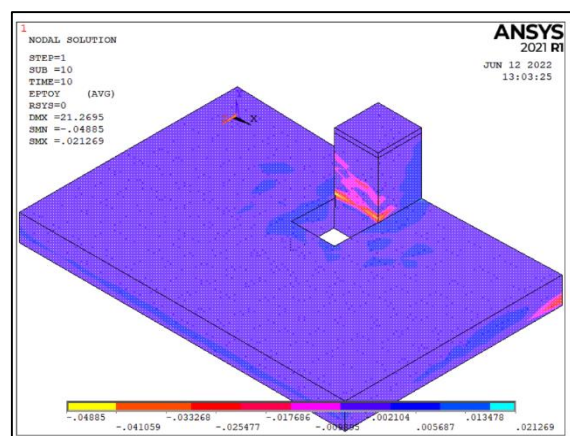


Fig. 20: principal Strain for specimen with one opening

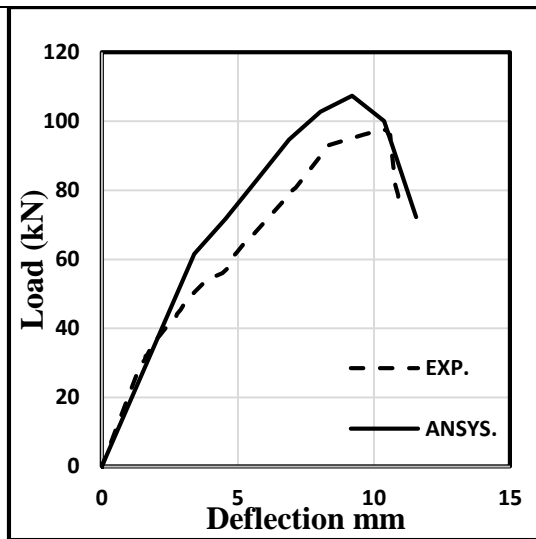


Fig. 21: Load – central deflection for specimen (S-A-O) with one opening

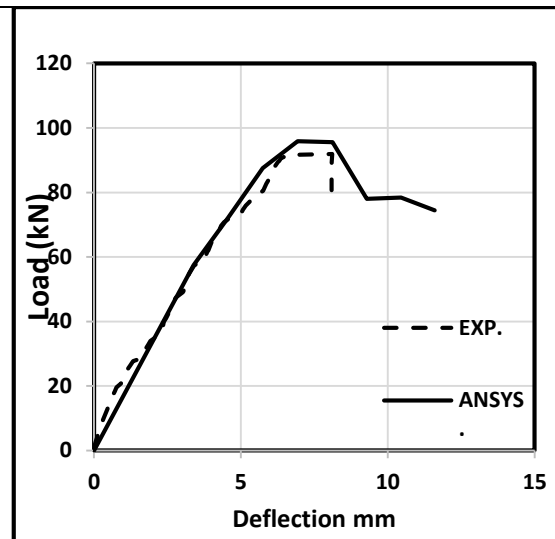


Fig. 22: Load – central deflection for specimen (S-A-2O) with two openings

9. Conclusions

The following points can be advanced based on experiments performed on two reinforced concrete slabs, including the number of apertures and the location of shear steel reinforcement, tested under vertical loads.

1. The presence of openings in a flat slab significantly reduces shear punching capacity and energy absorption.
2. Creating an opening at the column face and increasing the opening dimension to a value greater than span/10 (the limit of Egyptian code) shows a high drop in punching shear resistance. Increasing opening numbers decreased ultimate failure, stiffness, and energy absorption.
3. Comparing the analytical results from ECP 203-2020 and ACI 318-19 to the experimental results showed lower values. In contrast, the American code achieves higher ultimate load values for slabs with two openings.
4. The experimental results were compared to the theoretical method (ANSYS v. 21), and the findings showed close similarity between them.

References:

1. Lapi, Massimo, António Pinho Ramos, and Maurizio Orlando. "Flat slab strengthening techniques against punching-shear." *Engineering Structures* 180 (2019): 160-180.
2. Setiawan, Andri, Robert L. Vollum, Lorenzo Macorini, and Bassam A. Izzuddin. "Punching of RC slabs without transverse reinforcement supported on elongated columns." In *Structures*, vol. 27, pp. 2048-2068. Elsevier, 2020.
3. Abu-Salma, Deema, Robert L. Vollum, and Lorenzo Macorini. "Modelling punching shear failure at edge slab-column connections by means of nonlinear joint elements." In *Structures*, vol. 34, pp. 630-652. Elsevier, 2021.

4. Sagaseta, Juan, Luca Tassinari, M. Fernández Ruiz, and Aurelio Muttoni. "Punching of flat slabs supported on rectangular columns." *Engineering Structures* 77 (2014): 17-33.
5. El-Shafiey, Tarek F., Ahmed M. Atta, Ali Hassan, and Mohamed Elnasharty. "Effect of opening shape, size and location on the punching shear behaviour of RC flat slabs." *In Structures*, vol. 44, pp. 1138-1151. Elsevier, 2022.
6. Anil, Özgür, Tolga Kina, and Vahed Salmani. "Effect of opening size and location on punching shear behaviour of two-way RC slabs." *Magazine of concrete research* 66, no. 18 (2014): 955-966.
7. Elsayed, Mahmoud, Bassam A. Tayeh, and Doaa Kamal. "Effect of crumb rubber on the punching shear behaviour of reinforced concrete slabs with openings." *Construction and Building Materials* 311 (2021): 125345.
8. Liberati, Elyson AP, Marília G. Marques, Edson D. Leonel, Luiz C. Almeida, and Leandro M. Trautwein. "Failure analysis of punching in reinforced concrete flat slabs with openings adjacent to the column." *Engineering Structures* 182 (2019): 331-343.
9. Genikomsou, Aikaterini S., and Maria Anna Polak. "Finite element analysis of punching shear of concrete slabs using damaged plasticity model in ABAQUS." *Engineering structures* 98 (2015): 38-48.
10. Mostofinejad, Davood, Navid Jafarian, Ali Naderi, Amirmahdi Mostofinejad, and Mohamad Salehi. "Effects of openings on the punching shear strength of reinforced concrete slabs." *In Structures*, vol. 25, pp. 760-773. Elsevier, 2020.
11. Teng, Susanto, H. K. Cheong, K. L. Kuang, and J. Z. Geng. "Punching shear strength of slabs with openings and supported on rectangular columns." *Structural Journal* 101, no. 5 (2004): 678-687.
12. Egyptian Reinforced Concrete Code Committee 203. *Egyptian code for design and construction of reinforced concrete structures (ECP203-2020)*. Giza, Egypt: Housing and Building National Research Center; 2020.
13. ACI Committee 318. *Building Code Requirement for Structural Concrete (ACI-318M-14) and Commentary (ACI 318RM-14)*. American Concrete Institute, 2014.
14. "ES 4756-1/2013, Egyptian Standard Specification "Cement - Part 1 Composition, Specification and Conformity Criteria for Common Cement"," Housing and Building Researching Center, Control, Egyptian Organization for Standard and Quality, Cairo-Egypt, 2013.
15. "ES 1109/2008, Egyptian Standard "Aggregates for Concrete"," Housing and Building Research Center, Control, Egyptian Organization for Standard and Quality, Cairo-Egypt, 2008.
16. E.A. Liberati, M.G. Marques, E.D. Leonel, L.C. Almeida, L.M. Trautwein, Failure analysis of punching in reinforced concrete flat slabs with openings adjacent to the column, *Engineering Structures*. 182 (2019) 331-343.
17. Ö. Anil, T. Kina, V. Salmani, Effect of opening size and location on punching shear behaviour of two-way RC slabs, *Magazine of Concrete Research*. 66, 18 (2014) 955-966